Lab on a Chip

Cite this: *Lab Chip*, 2012, **12**, 2069–2073

www.rsc.org/loc

PAPER

Monitoring the hydration of DNA self-assembled monolayers using an extensional nanomechanical resonator

Alberto Cagliani,*[a] Priscila Kosaka,[b] Javier Tamayo[b] and Zachary James Davis[a]

Received 10th January 2012, Accepted 16th March 2012
DOI: 10.1039/c2lc40047b

We have fabricated an ultrasensitive nanomechanical resonator based on the extensional vibration mode to weigh the adsorbed water on self-assembled monolayers of DNA as a function of the relative humidity. The water adsorption isotherms provide the number of adsorbed water molecules per nucleotide for monolayers of single stranded (ss) DNA and after hybridization with the complementary DNA strand. Our results differ from previous data obtained with bulk samples, showing the genuine behavior of these self-assembled monolayers. The hybridization cannot be inferred from the water adsorption isotherms due to the low hybridization efficiency of these highly packed monolayers. Strikingly, we efficiently detect the hybridization by measuring the thermal desorption of water at constant relativity humidity. This finding adds a new nanomechanical tool for developing a label-free nucleic acid sensor based on the interaction between water and self-assembled monolayers of nucleic acids.

1. Introduction

Nanomechanical resonators exhibit very high sensitivity for measuring small masses. The concept is simple, as the dynamic behavior of these resonators can closely be described by the damped harmonic oscillator model; a tiny mass deposited on the vibrating region of the device gives rise to a significant shift of the resonance frequency to a lower frequency. Since the frequency shift is inversely proportional to the active mass of the resonator, the miniaturization of the resonator by means of micro- and nanofabrication techniques brings to unprecedented mass resolutions. During the past five years mass resolutions from attograms to zeptograms have been reported.[1–5] Normally, these measurements are performed with singly or doubly clamped micro- or nanobeams in high vacuum environments where the viscous damping is minimized, and hence the quality factors range from 1000 to 100 000. The implementation of these devices for measurements in ambient conditions and liquids have been hindered by the viscous damping that reduces the quality factor and the sensitivity by at least two orders of magnitude.[6–9] Measurements in these environments are required in a wide variety of problems in materials and life science, such as polymer properties, gas sensing, corrosion, mechanical testing of thin coatings, biological interactions, to name a few.[10] Another difficulty of the use of singly or doubly clamped resonant beams is that the mass and mechanical properties of the adsorbate can both influence the resonant frequency in opposite directions, which degrades the sensitivity and complicates the interpretation of the measurement.[1,11–14]

Recently, advances in micro- and nanofabrication have provided micromechanical resonators based on the extensional vibration modes for a variety of mechanical geometries.[15,16] These devices have fully integrated electrical readout and actuation, and exhibit resonant frequencies of at least tens of MHz that increase the sensitivity in the frequency response to added mass.[17,18] However, the most important feature is that extensional vibration modes exhibit significantly smaller viscous damping than the flexural vibration modes of beams, and therefore can be applied for measurements in ambient conditions.[17,18] In addition, since these resonators are usually thicker than the resonant beams used in mass sensing, the mechanical effect of the adsorbate is minimized, and the frequency signal can be readily interpreted in terms of adsorbed mass.

Here, we have fabricated a longitudinal bulk acoustic nanomechanical resonator (LBAR) to obtain further insight on the hydration of self-assembled monolayers of DNA. In physiological conditions, the arrangement of the water molecules and counter ions near the DNA strongly influences its mechanical stability, conformation and interactions.[19–21] In addition, the hydration effect on the conformation of DNA self-assembled monolayers on gold has been used for label-free sensing of nucleic acids.[22] However, little is still known about the interaction between the water molecules and DNA and its role in fundamental life processes (such as replication, transcriptions, condensation and interaction with proteins) as well as in biosensing application.[20,21] A difficulty in studying the DNA–water interactions is that the properties of the hydration shells are strongly masked by the bulk water. A second difficulty is that

[a]*DTU-Nanotech, Ørsted Plads building 345, Kgs. Lyngby, Denmark. E-mail: Alberto.Cagliani@nanotech.dtu.dk; Tel: 004545255759*
[b]*IMM-Instituto de Microelectrónica de Madrid (CNM-CICS), Isaac Newton 8 PTM, E-28760, Tres Cantos, Spain*

water is a very light molecule that only weighs 30 yoctograms (1 yoctogram = 10^{-24} g), and hence it is hardly detectable. Advantageously, the hydration shells retain their identity in ambient conditions, and therefore the water–DNA interactions can be studied in ambient conditions. In this work, we use LBARs in an environmental chamber that enables the control of the temperature and the humidity of the resonator near environment to study the interaction of water with self-assembled DNA monolayers on gold.

2. Results

2.1 Longitudinal bulk acoustic mechanical microresonator (LBAR) characterization

A scanning electron microscopy image of the resonator is shown in Fig. 1a. The device is operated in a longitudinal extensional mode, as shown in Fig. 1b where the two cantilevers constituting the resonator are moving along the length in antiphase motion.[18] This mode is actuated electrostatically and the resulting resonance frequency is detected by capacitive readout between the two electrodes and the resonator, as shown in Fig. 1c. The resonance frequency of the LBAR used in this work is 49.16 MHz and the Q-factor in dry air (r.h. $<$ 2%) at room temperature is about 3300. For applications where the added mass creates a uniform layer on the surface of the sensor, as in this work, the parameter that defines the device responsivity is the frequency shift divided by the added mass per unit area. The responsivity of our LBARs was determined experimentally by measuring the resonance frequency shift after the evaporation of a 2 nm thick chromium (Cr) adhesion layer and 20 nm thick gold (Au) layer onto the microresonators. From the measurement of 18 different resonators, we obtained a responsivity of 1.69 $\pm$ 0.1 kHz μm^2 fg^{-1}. This value is used to calculate the masses corresponding to the water adsorption and desorption on the DNA films (Fig. 1d). The frequency noise in the experiments was 50 Hz, giving rise to a mass resolution of 30 attograms μm^{-2}. Since the mass density of a water monolayer on a surface is around 200–300 attograms μm^{-2}, the device is able to detect the formation of water submonolayers.

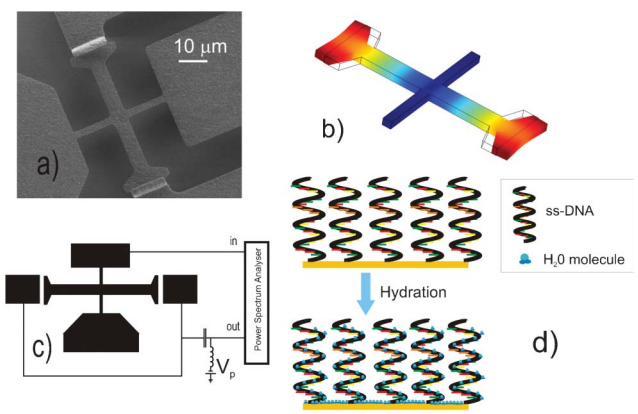

Fig. 1 (a) SEM micrograph of the LBAR resonator used for the experiments. The resonator is anchored at the center and two electrodes are placed close to the ends separated by a narrow air gap. (b) First extensional mode shape in which the device is driven into resonance. (c) Electrical scheme used to measure the resonant signals. (d) Illustration of the ssDNA SAM hydration.

2.2 Adsorption of water on DNA self-assembled monolayers

The LBARs frequencies were measured before and after the immobilization of a 16 mer ssDNA derivatized with a thiol linker at the 5′-end to form a self-assembled monolayer on the gold surface. We observe a decrease of the resonance frequency of 5 $\pm$ 1 kHz. From this value, a surface density of about 3.34 $\times$ 10^{13} chains cm^{-2} was deduced. The obtained surface density is in agreement with previous reports and indicates that most of the molecules are in the standing-up conformation.[22–25] After the ssDNA immobilization, the microresonators were placed inside an environmental chamber that allows the control of the relative humidity and the temperature. In Fig. 2a the adsorption isotherms for the gold-coated and ssDNA functionalized resonators are shown for a relative humidity from 2% to 65%. The error bars arise from the standard deviation of the isotherms between different resonators. The isotherms for the hybridized DNA surfaces were also acquired, but they were indistinguishable within the measurement error, which indicates that the hybridization yield is very low, otherwise an increase of DNA bases would lead to a higher number of adsorbed water molecules. This is consistent with previous reports that have shown that less than 10% of the immobilized probes are free to hybridize at our high immobilization density, because of steric

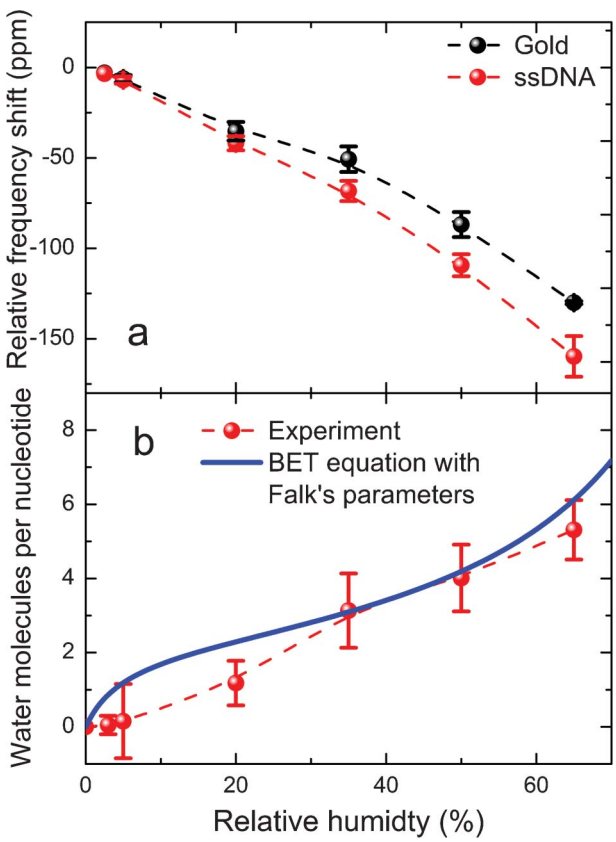

Fig. 2 (a) Adsorption isotherms for the gold-coated surface and the ssDNA functionalized resonators; (b) number of water molecules per nucleotide for the ssDNA functionalized surface (spheres) and a plot of the BET equation using Falk's parameters (blue line).

crowding, electrostatic repulsion between neighboring surface species, and nonspecific adsorption of thiolated probes *via* polar side groups.[26–28] The isotherm for the gold surface lies below the ssDNA isotherm, which indicates that the DNA monolayer adsorbs more water molecules than the gold surface. The water forms a monolayer on the gold (111) surfaces for a relative humidity of about 65%,[29] whereas the ssDNA monolayer, in addition to the unbound gold atoms, provides multiple binding sites along the single strand DNA chain supporting up to 6 water molecules per nucleotide at 65% relative humidity, excluding the 2 or 3 water molecules tightly bound to the phosphate skeleton even at 0% r.h. (Fig. 1d).[30]

Since the water is adsorbed in all the regions of the resonator, the two isotherms were subtracted in order to obtain just the contribution from the functionalized area. From the sensor calibration and the obtained DNA immobilization density, we obtain the number of water molecules per nucleotide from the differential measurement (Fig. 2b). The water uptake by DNA as a function of the relative humidity has extensively been studied in samples consisting of macroscopic fibers of long DNA obtained by standard desiccation methods. These samples consist of DNA with lengths of hundreds of nm arranged in bundles of fibers ~3 μm in diameter. Each fiber is composed of nanocrystallites with the DNA helical axis well aligned that are approximately 20 nm in diameter and macroscopic in length.[31] In these studies firstly established by Falk and collaborators,[32] the water adsorption isotherms closely follow the Brunauer–Emmett–Teller (BET) equation,

$$A = \frac{BCx}{(1-x)(1-x+Cx)} \quad (1)$$

where, A is the total amount of water adsorbed at relative humidity x, B is maximum number of water molecules accommodated on the primary adsorption sites and C is a constant given by

$$C = \exp\left(\frac{E_1 - E_L}{kT}\right) \quad (2)$$

The constants E_1 and E_L are the adsorption energies for the first layer and successive layers, respectively. The parameters that fit the experiments with macroscopic DNA fibers are B = 2.2 and C = 20, approximately.[30,32,33] The measurements and the theory do not include the structural 0th hydration layer that contains 2.5–3 water molecules strongly bound to each nucleotide that cannot be removed by typical drying methods.[30,33] We have also plotted the BET equation with Falk's parameters in Fig. 2b. We find that our data significantly falls below the Falk's data at humidity below 35%. This difference is not unexpected if one accounts for the significant structural differences between our sample and the macroscopic DNA fibers. Our sample is a highly packed two-dimensional monolayer of mostly standing 6 nm long DNA strands that are strongly anchored to the surface *via* the sulfur–gold linkage. The gap between neighbouring ssDNA molecules is about 0.8 nm and can host between two and three water layers. It may be expected that the interhelical bonding interactions hampers the water penetration in the monolayer at low humidity explaining the lower water uptake. Notice that in addition to the difference in structure, order and size, the DNA macrofibers are not geometrically constrained to accommodate the adsorbed water, *i.e.*, the sample swells with the humidity. In our case, the strong attachment of the DNA to the surface gives rise to an additional steric restriction to accommodate the excess of water.

Given the general good agreement of our adsorption data and the Falk's data, we believe that the well studied water molecule shell structure is also valid for our samples. Previous studies indicate that the water adsorption isotherm shown in Fig. 2b is related to the adsorption of water molecules belonging to the primary hydration shell that surrounds the DNA molecules in physiological conditions.[21,30,34,35] The primary hydration shell consists of ~10 water molecules per nucleotide, from which six are tightly bound at the ionic phosphate groups because of its high affinity for water. In our experiments, we observe the completion of the hydration of the phosphate groups at ~65% relative humidity.

2.3 Water desorption induced by heat transfer

In order to obtain further insight on the thermodynamics of the water adsorption on DNA self-assembled monolayers, we applied temperature ramps at room temperature of ~7 °C at constant relative humidity. Fig. 3a shows the typical response of the resonance frequency of a bare gold-coated resonator and a ssDNA functionalized resonator at 50% relative humidity. In

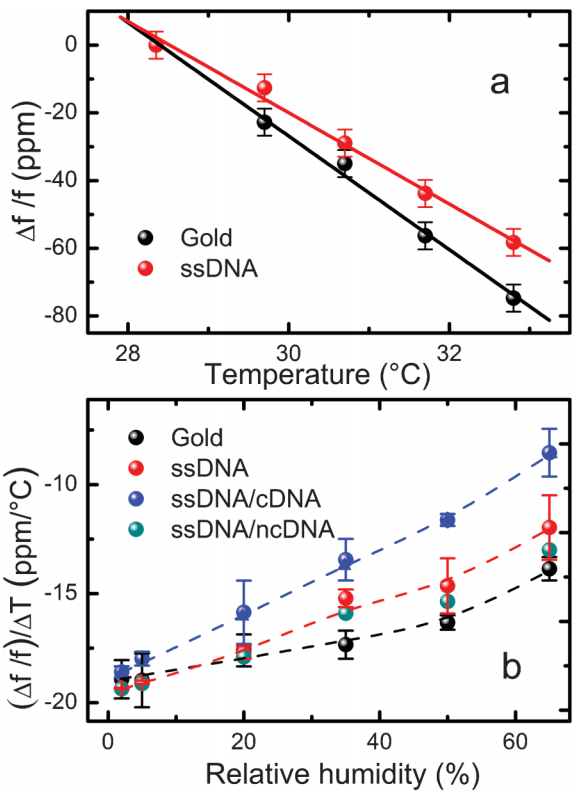

Fig. 3 (a) Typical response of the resonance frequency for the gold-coated surface and the ssDNA resonator at 50% relative humidity; (b) temperature dependency of the slopes of the resonance frequency *vs.* temperature curves at several values of relative humidity for the gold-coated surface, ssDNA functionalized resonator, after subsequent reactions with the non-complementary DNA (ssDNA/ncDNA) and complementary DNA (ssDNA/cDNA).

both cases, the resonance frequencies of the devices decrease with the temperature, however, this decrease is significantly smaller for the ssDNA-coated resonator. The response of the resonator to the temperature increase is a result of two competing effects; one is the decrease of the Young's modulus of the polysilicon that is about −46 ppm °C^{-1} which leads to a decrease of the resonance frequency with the temperature;[36] the other is the thermal desorption of the water adsorbed on the resonator that leads to an increase of the resonance frequency. Consistent with the adsorption isotherms shown in Fig. 2a, a higher amount of water evaporates from the ssDNA functionalized resonators. The resonance frequency linearly changes within the used temperature range, and thereby the frequency *vs.* temperature curves can be well-fitted with a linear curve. We plot the slopes of the linear fittings in Fig. 3b at several values of relative humidity for the gold-coated resonator, for the ssDNA functionalized resonator, before and after the subsequent reactions with complementary and non-complementary DNA. In all the curves, the slope decreases with the humidity as a consequence of the higher water evaporation. The ssDNA shows higher thermal desorption than the gold surface, in particular for relative humidity values above 20%. After incubation of the resonator with non-complementary DNA, there is not a significant change in the curves. However, the hybridization with the complementary DNA sequence gives rise to a drastic increase in the amount of thermal water desorption.

In order to highlight the contribution of the water evaporation, we subtract the data of the gold-coated resonator from the data of the DNA-coated resonators. Fig. 4 shows the number of thermally desorbed water molecules per nucleotide and per Celsius degree for a ssDNA coated resonator and after subsequent hybridization with the complementary sequence. The amount of desorption increases with the humidity as expected, since the number of water molecules bound to the DNA also increases. The most striking aspect is that the hybridization dramatically increases the amount of thermal desorption at all values of relative humidity. This result is unexpected if one takes into account the low hybridization yield and that the hybridization cannot be inferred from the adsorption isotherms. This means this effect cannot be attributed simply to a higher amount of water on the surface. Therefore, it is clear that the water molecules are significantly more loosely bound to the hybridized DNA surface, thus showing a lower desorption barrier. As mentioned above, we attribute this finding to the high grafting density of the self-assembled monolayers of ssDNA that gives rise to steric crowding repulsive interactions with other molecules in their attempt to penetrate into the monolayer, as occurs with the water and complementary DNA molecules. After hybridization the average spacing gap between the DNA molecules is significantly smaller, and it is expected a reduction in the water desorption energy due to the higher steric barrier. In addition, the hydrogen bond network is more disrupted as a consequence of the higher degree of confinement.[24] Due to the novelty of these results no references related to the desorption barrier on DNA monolayers was found in the literature. More research work has to be carried out to fully explain these results; in any case, a strong indication of the reduction of the desorption barrier for water has been observed. A closely related research work has shown a similar effect. In fact, it was observed by Mertens *et al.* on measurements of the surface stress *vs.* humidity in DNA functionalized microcantilevers[22] that the pattern of these curves dramatically changed after hybridization, even at very low concentrations of the complementary sequence.

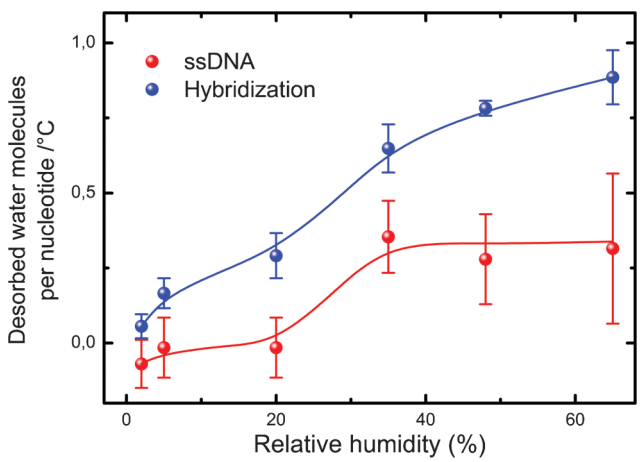

Fig. 4 Number of thermally desorbed water molecules per nucleotide and per °C as a function of the relative humidity for ssDNA functionalized resonator and after hybridization with the complementary sequence.

3. Experimental section

3.1 Longitudinal bulk acoustic mechanical microresonator

The longitudinal bulk acoustic micromechanical resonator (LBAR) used in this work consists of a polysilicon bar 60 μm in length electrostatically driven into resonance. The microfabrication process used to fabricate the LBAR is described in ref. 17. The output signal is due to the change in the capacitance between the charged vibrating bar and the electrodes.[17] An Agilent Spectrum Analyzer N9320 (9 kHz–3.0 Ghz) , combined with a low noise dc power supply PL601-P (60 V, 1.5 A) from Aim TTi Instruments (represented by V_p in Fig. 1c) have been used to measure the resonant signals.

3.2 DNA immobilization and hybridization

Commercial purified oligonucleotides were obtained from Stab Vida (Portugal). DNA oligomers were HPLC purified and desiccated. The oligonucleotide sequences used in this work were the thiol-modified 16-mer probe 5′-HS-CTACCTTTTTTT-TCTG-3′, the fully complementary target (5′-CAGAAAAA-AAAGGTAG-3′) and the non-complementary target used as a negative hybridization control (5′-AGCTTCCGTACTCGAT-3′). Prior to use, the samples were resuspended in PBS buffer with 1 M NaCl (pH 7.5) and divided in aliquots of the desired volume and concentration without further modification. All solutions were prepared using DNase/RNase free water from Sigma-Aldrich and stored at −20 °C.

The resonators were coated by e-beam evaporation with a 2 nm Cr adhesion layer and a 20 nm Au layer at a deposition rate of 0.2 Å s^{-1}. Freshly coated resonators were incubated with 5 μM of the thiol-modified single stranded DNA probe (ssDNA)

at room temperature and under gentle agitation for 36 h in order to immobilize a densely packed DNA layer. After immobilization, each sample was rinsed sequentially with PBS buffer with 1 M NaCl and DNase/RNase free water to discard unspecific interactions. Afterwards, the resonators were dipped into isopropanol to avoid the collapse of the resonator and then dried under a stream of dry N_2 gas. The hybridization of the functionalized resonator with the complementary sequence was performed in PBS with 1 M NaCl at room temperature and under agitation for 2–4 h. Solutions for control and hybridization experiments contained 1 μM target DNA.

3.3 Measurement of the DNA layers hydration

After DNA immobilization and hybridization, the microresonators were placed inside an environmental chamber where the relative humidity (r.h.) and the temperature (T) of the resonator could be controlled during all of the experiment. The temperature was controlled by means of a Peltier cell placed right below the resonator, with a temperature sensor close to it. The r.h. in the environmental chamber was controlled by mixing dry nitrogen (N_2) and wet nitrogen (dry N_2 bubbling through a glass bottle filled with fresh Milli-Q water) using precision valves. The humidity was changed within a working range from 2% up to 65% with a resolution of 0.1%, while the temperature of the resonator was controlled using closed loop electronics with a resolution of 0.1 °C. Prior to the measurement and to ensure that the microresonator surface was completely dry before starting the experiment, the resonators were equilibrated below r.h. 2% for several hours.

Conclusions

In this work, we demonstrate the potential of a longitudinal bulk acoustic nanomechanical resonator for weighing minute masses in ambient conditions. In particular, we have measured the added mass due to water adsorption on self-assembled monolayers of DNA. The data presented shed light on the interaction between water and DNA molecules. This interaction plays a critical role in the function, interactions, and conformation of DNA in physiological conditions as well as in biosensing. We have found that the amount of thermal desorption of water molecules is significantly higher after hybridization of the monolayer. This remarkable difference can be used as a hybridization fingerprint in future label-free sensors of nucleic acids.

Acknowledgements

The authors acknowledge financial support from the Spanish Science Ministry through the project TEC2009-14517-C02-02. They also acknowledge Dr Sheila Gónzalez by her technical support in the atomic force microscopy measurements. They also acknowledge Valerio Pini for the very fruitful discussion on the temperature dependence of the devices used.

References

1 E. Gil-Santos, D. Ramos, J. Martínez, M. Fernández-Regúlez, R. García, Á. San Paulo, M. Calleja and J. Tamayo, *Nat. Nanotechnol.*, 2010, **5**, 641–645.
2 A. Naik, M. Hanay, W. Hiebert, X. Feng and M. Roukes, *Nat. Nanotechnol.*, 2009, **4**, 445–450.
3 Y. Yang, C. Callegari, X. Feng, K. Ekinci and M. Roukes, *Nano Lett.*, 2006, **6**, 583–586.
4 K. Ekinci, Y. Yang and M. Roukes, *J. Appl. Phys.*, 2004, **95**, 2682.
5 M. Varshney, P. S. Waggoner, C. P. Tan, K. Aubin, R. A. Montagna and H. G. Craighead, *Anal. Chem.*, 2008, **80**, 2141–2148.
6 T. P. Burg, M. Godin, S. M. Knudsen, W. Shen, G. Carlson, J. S. Foster, K. Babcock and S. R. Manalis, *Nature*, 2007, **446**, 1066–1069.
7 M. K. Ghatkesar, V. Barwich, T. Braun, A. Bredekamp, U. Drechsler, M. Despont, H. Lang, M. Hegner and C. Gerber, *IEEE Sens. 2004*, 2004, **2**, 1060–1063.
8 D. Ramos, J. Mertens, M. Calleja and J. Tamayo, *Appl. Phys. Lett.*, 2008, **92**, 173108.
9 T. Braun, M. K. Ghatkesar, N. Backmann, W. Grange, P. Boulanger, L. Letellier, H. P. Lang, A. Bietsch, C. Gerber and M. Hegner, *Nat. Nanotechnol.*, 2009, **4**, 179–185.
10 M. Yun, N. Jung, C. Yim and S. Jeon, *Polymer*, 2011, **52**, 4136–4140.
11 D. Ramos, M. Arroyo-Hernandez, E. Gil-Santos, H. Duy Tong, C. Van Rijn, M. Calleja and J. Tamayo, *Anal. Chem.*, 2009, **81**, 2274–2279.
12 R. Grüter, Z. Khan, R. Paxman, J. Ndieyira, B. Dueck, B. Bircher, J. Yang, U. Drechsler, M. Despont and R. McKendry, *Appl. Phys. Lett.*, 2010, **96**, 023113.
13 D. Ramos, J. Tamayo, J. Mertens, M. Calleja and A. Zaballos, *J. Appl. Phys.*, 2006, **100**, 106105.
14 J. Tamayo, D. Ramos, J. Mertens and M. Calleja, *Appl. Phys. Lett.*, 2006, **89**, 224104.
15 T. Mattila, J. Kiihamaki, T. Lamminmaki, O. Jaakkola, P. Rantakari, A. Oja, H. Seppa, H. Kattelus and I. Tittonen, *Sens. Actuators, A*, 2002, **101**, 1–9.
16 J. E. Y. Lee and A. Seshia, *Sens. Actuators, A*, 2009, **156**, 28–35.
17 A. Cagliani and Z. Davis, *J. Micromech. Microeng.*, 2011, **21**, 045016.
18 J. H. Hales, J. Teva, A. Boisen and Z. J. Davis, *Appl. Phys. Lett.*, 2009, **95**, 033506.
19 J. Mertens, J. Tamayo, P. Kosaka and M. Calleja, *Appl. Phys. Lett.*, 2011, **98**, 153704.
20 J. Barciszewski, J. Jurczak, S. Porowski, T. Specht and V. A. Erdmann, *Eur. J. Biochem.*, 1999, **260**, 293–307.
21 H. M. Berman, *Curr. Opin. Struct. Biol.*, 1991, **1**, 423–427.
22 J. Mertens, C. Rogero, M. Calleja, D. Ramos, J. A. Martín-Gago, C. Briones and J. Tamayo, *Nat. Nanotechnol.*, 2008, **3**, 301–307.
23 L. Dongsheng and S. Wenmiao, Microcantilever Biosensors: Probing Biomolecular Interactions at the Nanoscale, *Curr. Org. Chem.*, 2011, **15**, 477–485.
24 M. F. Hagan, A. Majumdar and A. K. Chakraborty, *J. Phys. Chem. B*, 2002, **106**, 10163–10173.
25 R. McKendry, J. Zhang, Y. Arntz, T. Strunz, M. Hegner, H. P. Lang, M. K. Baller, U. Certa, E. Meyer and H. J. Güntherodt, *Proc. Natl. Acad. Sci. U. S. A.*, 2002, **99**, 9783.
26 R. Levicky, T. M. Herne, M. J. Tarlov and S. K. Satija, *J. Am. Chem. Soc.*, 1998, **120**, 9787–9792.
27 T. M. Herne and M. J. Tarlov, *J. Am. Chem. Soc.*, 1997, **119**, 8916–8920.
28 K. A. Peterlinz, R. M. Georgiadis, T. M. Herne and M. J. Tarlov, *J. Am. Chem. Soc.*, 1997, **119**, 3401–3402.
29 A. Gil, J. Colchero, M. Luna, J. Gómez-Herrero and A. Baró, *Langmuir*, 2000, **16**, 5086–5092.
30 N. Tao, S. Lindsay and A. Rupprecht, *Biopolymers*, 1989, **28**, 1019–1030.
31 S. Lee, S. Lindsay, J. Powell, T. Weidlich, N. Tao, G. Lewen and A. Rupprecht, *Biopolymers*, 1987, **26**, 1637–1665.
32 M. Falk, K. A. Hartman and R. Lord, *J. Am. Chem. Soc.*, 1962, **84**, 3843–3846.
33 N. Armitage, M. Briman and G. Grüner, *Phys. Status Solidi B*, 2004, **241**, 69–75.
34 N. Tao, S. Lindsay and A. Rupprecht, *Biopolymers*, 1988, **27**, 1655–1671.
35 B. Schneider and H. M. Berman, *Biophys. J.*, 1995, **69**, 2661–2669.
36 W. T. Hsu, J. R. Clark and C. T. C. Nguyen, *Electron Devices Meeting*, 2000, 399–402.